Supplemental material for "Speed-dependent adaptive partitioning in QM/MM MD simulations of displacement damage in solid-state systems"

Zeng-hui Yang*,†,‡

Microsystem and Terahertz Research Center, China Academy of Engineering Physics, Chengdu, China 610200, and Institute of Electronic Engineering, China Academy of Engineering Physics, Mianyang, China 621000

E-mail: yangzenghui@mtrc.ac.cn

Abstract

This supplemental material contains the equation of motion derived from Lagrangian dynamics that conserves the SDAC Hamiltonian, implementation details of the EPS time-integration algorithm, and the comparison between the SDAC QM/MM calculation and the pure QM calculation.

1 EOM derived from Lagrangian dynamics

The Lagrangian EOM that conserves the Hamiltonian [Eq. (8) of main text] is

$$m_\alpha \vec{a}_\alpha = -\nabla_{\vec{r}_\alpha} V + \sum_\beta \left(\nabla_{\vec{r}_\beta} \cdot \nabla_{\vec{v}_\alpha} V\right) \vec{v}_\beta + \sum_\beta \left(\nabla_{\vec{v}_\beta} \cdot \nabla_{\vec{v}_\alpha}\right) \vec{a}_\beta. \quad (1)$$

The speed-dependence of Eq. (1) is more complicated than that of Eq. (9) of main text. Since all atoms are coupled together in Eq. (1), it is difficult to estimate the deviation of the dynamics described by Eq. (1) from that of the 'real system'.

2 Details of the EPS algorithm

The original phase space at the initial time is $\left(\{\vec{r}_\alpha^{(0)}\}, \{\vec{v}_\alpha^{(0)}\}\right)$, in which I use velocities instead of momenta for simpler notation. In the EPS algorithm, the original phase space is duplicated to form an extended phase space $(\{\vec{r}_\alpha\}, \{\vec{v}_\alpha\}, \{\vec{r}_\alpha{}'\}, \{\vec{v}_\alpha{}'\})$. The time integration is performed in the extended phase space, and the original phase space of a certain time step is obtained from the extended phase space by projection. One can choose to carry out the time integration entirely in the extended phase space, or project back to the original phase space and form the extended phase space with the projected values after a few steps. The EPS time propagation operator that run in the extended phase space for k time steps can be written as:[1]

$$\Psi^{(k)} = \hat{P} \circ \left[\hat{M}_2 \hat{R} \hat{V}' \hat{R}' \hat{V} \hat{M}_1 \hat{V} \hat{R}' \hat{V}' \hat{R}\right]^k \circ \hat{C}, \quad (2)$$

so that

$$\Psi^{(k)} \left(\{\vec{r}_\alpha^{(i)}\}, \{\vec{v}_\alpha^{(i)}\}\right) = \left(\{\vec{r}_\alpha^{(i+k)}\}, \{\vec{v}_\alpha^{(i+k)}\}\right). \quad (3)$$

The propagators $\hat{R}$, $\hat{V}$, $\hat{R}'$, and $\hat{V}'$ of Eq. (2) perform update to $\{\vec{r}_\alpha\}$, $\{\vec{r}_\alpha{}'\}$, $\{\vec{v}_\alpha\}$, and $\{\vec{v}_\alpha{}'\}$ re-

*To whom correspondence should be addressed

†Microsystem and Terahertz Research Center, China Academy of Engineering Physics, Chengdu, China 610200

‡Institute of Electronic Engineering, China Academy of Engineering Physics, Mianyang, China 621000

spectively:

$$\hat{R}: \quad \vec{r}_\alpha \leftarrow \vec{r}_\alpha + (\Delta t/2)\vec{v}_\alpha, \tag{4}$$

$$\hat{V}: \quad \vec{v}_\alpha \leftarrow \vec{v}_\alpha + (\Delta t/2)\vec{a}_\alpha(\vec{r}_\alpha, \vec{v}_\alpha{}'), \tag{5}$$

$$\hat{R}': \quad \vec{r}_\alpha{}' \leftarrow \vec{r}_\alpha{}' + (\Delta t/2)\vec{v}_\alpha{}', \tag{6}$$

$$\hat{V}': \quad \vec{v}_\alpha{}' \leftarrow \vec{v}_\alpha{}' + (\Delta t/2)\vec{a}_\alpha(\vec{r}_\alpha{}', \vec{v}_\alpha), \tag{7}$$

where Δt is the size of the time step.

$\hat{C}$ of Eq. (2) is the operator that extend the original phase space into the extended phase space:

$$\hat{C}\left(\{\vec{r}_\alpha^{(i)}\}, \{\vec{v}_\alpha^{(i)}\}\right) = \left(\{\vec{r}_\alpha^{(i)}\}, \{\vec{v}_\alpha^{(i)}\}, \{\vec{r}_\alpha^{(i)}\}, \{\vec{v}_\alpha^{(i)}\}\right) \tag{8}$$

The mixing operators $\hat{M}_n$ ($n = 1,2$) of Eq. (2) mixes the two parts of the extended phase space to improve the stability of the algorithm:

$$\begin{aligned}&\hat{M}_n\left(\{\vec{r}_\alpha\}, \{\vec{v}_\alpha\}, \{\vec{r}_\alpha{}'\}, \{\vec{v}_\alpha{}'\}\right) = \\ &\left(\{a_n\vec{r}_\alpha + (1-a_n)\vec{r}_\alpha{}'\}, \{b_n\vec{v}_\alpha + (1-b_n)\vec{v}_\alpha{}'\}, \right. \\ &\left.\{(1-a_n)\vec{r}_\alpha + a_n\vec{r}_\alpha{}'\}\}, \{(1-b_n)\vec{v}_\alpha + b_n\vec{v}_\alpha{}'\}\right).\end{aligned} \tag{9}$$

The projection operator $\hat{P}$ of Eq. (2) projects the extended phase space to the original phase space:

$$\begin{aligned}&\hat{P}\left(\{\vec{r}_\alpha\}, \{\vec{v}_\alpha\}, \{\vec{r}_\alpha{}'\}, \{\vec{v}_\alpha{}'\}\right) = \\ &\left(\{a\vec{r}_\alpha + (1-a)\vec{r}_\alpha{}'\}, \{b\vec{v}_\alpha + (1-b)\vec{v}_\alpha{}'\}\right).\end{aligned} \tag{10}$$

Different choices of the mixing and projection parameters of the EPS algorithm are available in the literature,[1–3] but they do not work well for the SDAC simulations and become unstable when the time step is larger than about 10^{-5} ps. This is due to that the QM/MM partitions of the two parts of the EPS may become different during the internal steps of the algorithm. I use $a_1 = a_2 = 1/2$, $b_1 = b_2 = 1/2$, $a = b = 1/2$ in this paper similar to Luo, et al.[4] Although the strong coupling between the two parts of the EPS by these parameters is considered undesirable in the original EPS paper,[1] these parameters allow the use of time steps much larger than 10^{-5} ps, which is needed for practical simulations.

The most computationally expensive step in the time-integration is the evaluation of the potential energy. The computational cost of the EPS algorithm per time step is therefore about 4 times larger than that of the velocity Verlet algorithm.

3 Comparison between the S-DAC QM/MM calculation and the pure QM calculation

In the main text, I show the validness of the S-DAC method by comparing the results of SDAC MM/MM calculations and pure MM calculations. Here I carry out a similar comparison between the SDAC QM/MM calculation and the pure QM calculation, with DFTB as the QM method and the SW potential as the MM method. Due to the restriction of the QM computational cost, I use a $4 \times 4 \times 4$ bulk Si supercell (512 atoms), which is much smaller than the systems in the main text. The lattice constant is fixed at 5.43Å. The initial velocity of the PKA is the same as in Sec. 3.2.2 of the main text (0.5 keV, 7° away from the z direction), and the velocities of all other atoms are set to 0 at $t = 0$. The DFTB calculation is carried out with a Γ-only k-grid to ensure that the result is directly comparable with the SDAC QM/MM result. The SDAC criterion property and the partition parameters are the same as in Sec. 3.2.2 of the main text (ξ^{full} with $R_{\max}^{\text{QM}} = 4$ Å, $\xi_{\min}^{\text{semi}} = 8$, $\xi_{\min}^{\text{QM}} = 9$, $\xi_{\max}^{\text{QM}} = 10$). NVE simulations are carried out with a time step of 5×10^{-6} ps for 0.05 ps, where the total simulation time is chosen to make sure that the PKA do not go across the periodic boundary of the system. The PKA is placed at the bottom of the system to make the simulation to run as long as possible. The SDAC simulation is run without transition forces.

Due to the small size of the system, the disordered regions spread across the periodic boundary (such as the two atoms seen at the top of Fig. fig:compareshape). This is taken into account in the calculation of $\langle dR \rangle$, $\langle dx \rangle / \langle dy \rangle$ and $\langle dx \rangle / \langle dz \rangle$. Nevertheless, the results shown in this section should be treated only as a verification of the SDAC method instead of proper simulations.

Fig. 1 compares various properties in the pure QM, SDAC QM/MM and pure MM calculations. Fig. 2 shows snapshots of the amorphous regions of these calculations at different time. The SDAC $v_{\max}$ closely follows the QM curve until

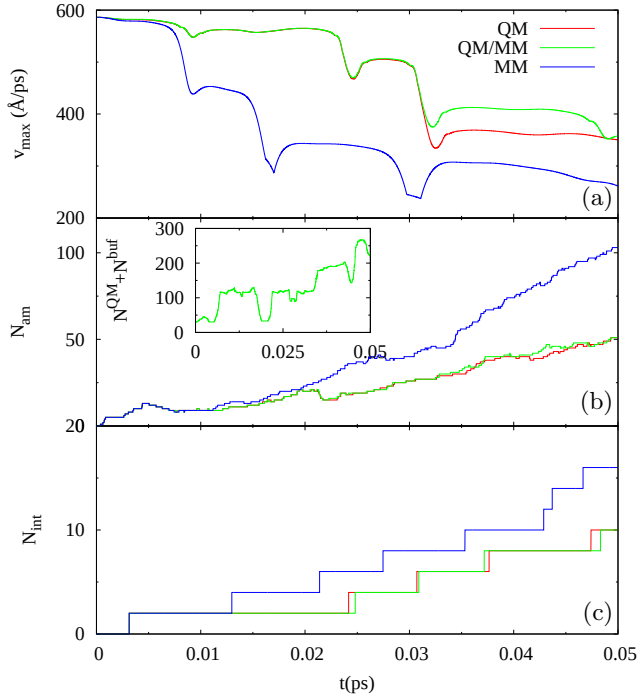

Figure 1: The max atomic speed, the number of atoms in amorphous regions, and the number of interstitials of the pure QM, SDAC QM/MM and pure MM calculations. The number of QM/buffer atoms of the SDAC QM/MM calculation is plotted in the inset.

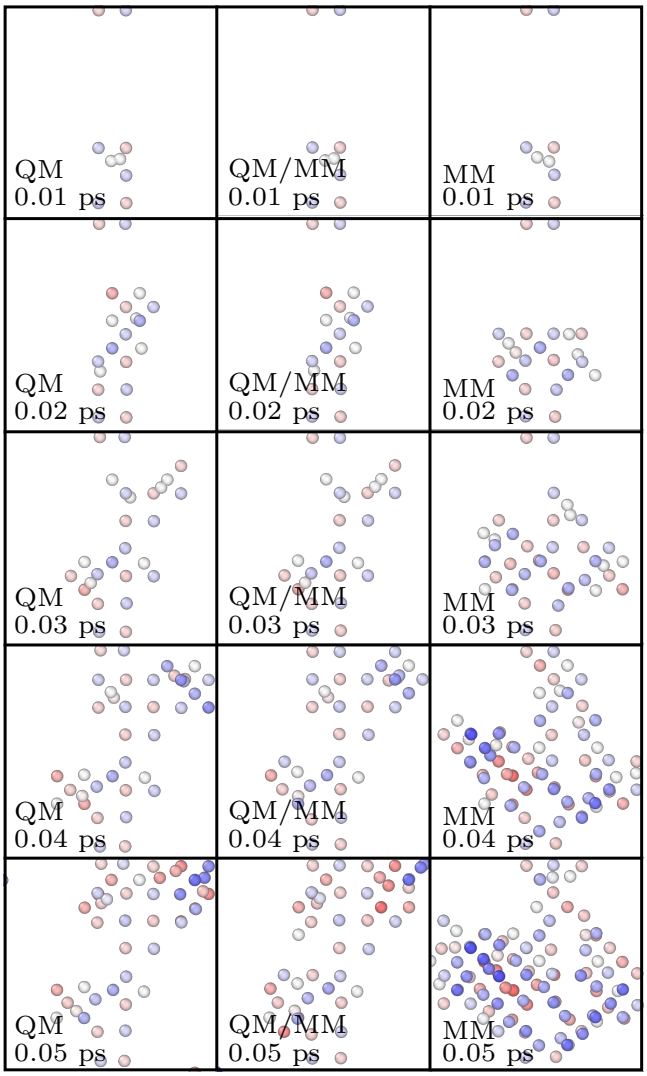

Figure 2: Front view (*xz* plane) snapshots of the amorphous pockets. The atoms in the amorphous regions are identified similarly as in the main text. The SDAC QM/MM calculation is carried out without transition forces. The blue-white-red color coding represent the *y* coordinate from small to large.

about 0.032 ps due to the difference in the specific trajectory of the PKA. This is also seen in Fig. 6(e) of the main text, where the ξ^{full} w/o F^{tr} curve is in general close to the Tersoff/ZBL curve but not completely the same. The SDAC QM/MM N_{am} and N_{int} curves in Fig. 1 remain very close after 0.032 ps. This and the snapshots in Fig. 2 confirm that the dynamics described by the SDAC method is very close to the pure QM reference, despite the dynamics described by the MM potential being drastically different, which is evident in Figs. 1 and 2 and Table 1.

Table 1: Morphology of the disordered regions in Fig. 2

Method	$\langle dR \rangle$ (Å)	$\langle dx \rangle / \langle dy \rangle$	$\langle dx \rangle / \langle dz \rangle$
$t = 0.01$ ps			
QM	3.527	1.011	0.3901
SDAC QM/MM	3.534	1.011	0.3913
MM	3.549	1.018	0.3984
$t = 0.02$ ps			
QM	5.159	1.038	0.3568
SDAC QM/MM	5.172	1.039	0.3586
MM	4.532	1.674	0.8280
$t = 0.03$ ps			
QM	6.415	2.140	0.5263
SDAC QM/MM	6.439	2.100	0.5278
MM	5.764	2.120	1.100
$t = 0.04$ ps			
QM	7.627	2.238	0.6744
SDAC QM/MM	7.668	2.195	0.6485
MM	7.026	1.772	1.094
$t = 0.05$ ps			
QM	8.261	1.872	0.7175
SDAC QM/MM	8.336	1.718	0.6958
MM	7.534	1.776	1.153

References

(1) Pihajoki, P. *Celest. Mech. Dyn. Astr.* **2015**, *121*, 211.

(2) Tao, M. *Phys. Rev. E* **2016**, *94*, 043303.

(3) Liu, L.; Wu, X.; Huang, G.; Liu, F. *Mon. Not. R. Astron. Soc.* **2016**, *459*, 1968.

(4) Luo, J.; Wu, X.; Huang, G.; Liu, F. *Astrophys. J.* **2017**, *834*, 64.